CrystEngComm

DOI: 10.1039/b000562m *CrystEngComm*, 2000, 4

The influence of ligand variation on the crystal properties of(η^4-azadiene)$Fe(CO)_{3-n}(PR_3)_n$ (*n* = 1, 2; R = Cy, Ph, OMe)†

Daniel Berger, Mandy Erdmann, Johannes Notni and Wolfgang Imhof*

Institut für Anorganische und Analytische Chemie der Friedrich-Schiller-Universität, August-Bebel-Str. 2, 07743 Jena, Germany. E-mail: cwi@rz.uni-jena.de

Received 19th January 2000, Accepted 8th February 2000, Published 11th February 2000

Compared to (η^4-azadiene)$Fe(CO)_3$ complexes the formal substitution of one or two CO ligands with phosphines or phosphites, respectively, leads to changes in the electronic structure of the organometallic compounds. The increased electron density at the iron atom brings about an out of plane position of H(C_3) of the azadiene chain which is necessary to stabilize the bonding between iron and C_3. The hydrogen atom is bent out of the plane of the azadiene ligand to a higher extend than in the corresponding $Fe(CO)_3$ derivatives. In all complexes with just one phosphorus containing ligand this ligand adopts the apical position in the square pyramidal coordination sphere of the iron atom. In addition, the number and nature of groups that may act as hydrogen donor or acceptor sites in intermolecular hydrogen bond systems building up the crystal structures is changed. The use of PCy_3 or PPh_3 mostly leads to the formation of dimers or chains by hydrogen bonding between the remaining CO ligands and C–H bonds either of the organic substituents of the azadiene or suitable C–H bonds of the organic moieties at the phosphine ligands. The use of one $P(OMe)_3$ leads to similar substructures which now are linked by additional hydrogen bonds involving both oxygen and hydrogen atoms of the phosphite ligands as hydrogen bond acceptor or donor sites. If two $P(OMe)_3$ ligands are present in the molecule the steric effect of these rather large ligands again leads to less complicated supramolecular architectures of the organometallic crystals which now in all cases occur as chains of dimers.

Introduction

Recently we reported the structural properties of a number of (1-azadiene)$Fe(CO)_3$ complexes.[1] We were interested in this class of compounds because there were only few reports on organic transformations known for complexed azadienes compared to the chemistry of 1,3-butadiene complexes.[2,3]

In all structural analyses we carried out on (1-azadiene)$Fe(CO)_3$ complexes we observed that in the coordinated ligand the H(C_3) hydrogen is found to be non-planar with respect to the C–C–C–N plane.[1] It has been demonstrated by means of extended Hückel calculations that this out of plane position of the 1-azadiene hydrogen atom H(C_3) has an electronic origin since it brings about better π*-backbonding between the 1-azadiene and $Fe(CO)_3$ molecular fragments.[1] The organometallic crystals showed the presence of a large number of hydrogen bond interactions of the C–H···O type involving CO-ligand acceptors. Hydrogen bonding of the azadiene moiety always involved the hydrogen atom at the C=N double bond and the hydrogen atom in the α-position with respect to the imine group but never with H(C_3) as the hydrogen donor site.[1]

On the other hand, (1-azadiene)$Fe(CO)_3$ complexes may well serve as model compounds for initial C–H activation steps during catalytic C–C coupling reactions starting from α,β-unsaturated imines.[4] These catalytic transformations show regioselective C–H activation reactions which for acyclic azadienes exclusively occur at C_3 of the azadiene chain, the same position that we found to exhibit special properties in the $Fe(CO)_3$ complexes due to the electronic reasons described above.

It has been pointed out before that CO ligands act as acceptor sites in hydrogen bond networks building up organometallic crystals.[5] Very recently also some high level calculations have been reported on the question whether the C–H···O interaction is a real hydrogen bond, which as a conclusion of this calculation was found to be true.[6] In this paper we describe the synthesis and the spectroscopical as well as structural properties of a number of iron azadiene complexes in which one or two CO ligands are substituted by various phosphorus containing ligands. By this variations we wanted to explore whether it is possible to induce distinct changes in the supramolecular architecture of the organometallic crystals by changing the number and properties of both hydrogen donor and acceptor sites in the molecule.

Synthesis and spectroscopic properties of the compounds

Scheme 1 shows the synthesis of the phosphine or phosphite substituted azadiene iron carbonyl complexes **1**–**15**. It is not possible to achieve the formation of **1**–**15** by reacting the corresponding (1-azadiene)$Fe(CO)_3$ complexes with the various phosphine ligands. This reaction always leads to substitution of the azadiene by the phosphines. So we had to use the phosphine substitution products of ironpentacarbonyl which may easily be prepared from $Fe(CO)_5$ and the corresponding phosphine under photochemical activation.[7] The reaction of $Fe(CO)_5$ with trimethylphosphite only gave the disubstitution product $Fe(CO)_3[P(OMe)_3]_2$. The 1-azadiene ligands we used were all prepared from cinnamaldehyde and various primary amines. If $Fe(CO)_4(PR_3)$ (R = Ph, Cy) is irradiated together with the azadiene ligands two CO ligands are replaced by the imine to produce **1**–**8**. The reaction of the azadienes with $Fe(CO)_3[P(OMe)_3]_2$ under the same reaction conditions leads either again to the substitution of two CO

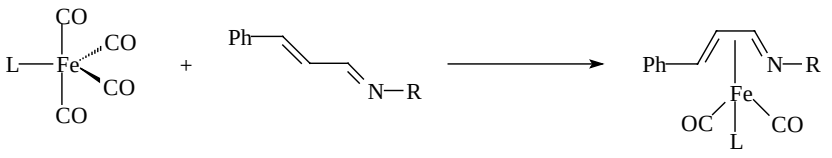

	L	R
1	PCy_3	Ph
2	PCy_3	4-Br-C_6H_4
3	PCy_3	4-CF_3-C_6H_4
4	PCy_3	Cy
5	PPh_3	Ph
6	PPh_3	4-Br-C_6H_4
7	PPh_3	4-CF_3-C_6H_4
8	PPh_3	Cy

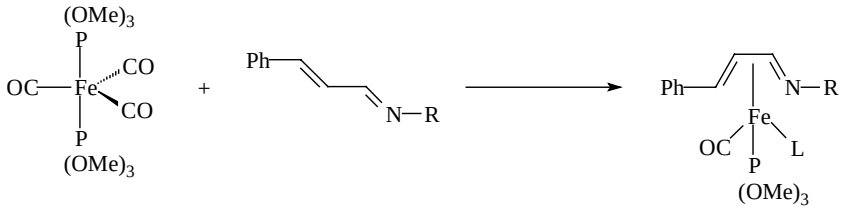

	L	R
9	CO	4-Br-C_6H_4
10	CO	4-CF_3-C_6H_4
11	CO	Cy
12	$P(OMe)_3$	Ph
13	$P(OMe)_3$	4-Br-C_6H_4
14	$P(OMe)_3$	4-CF_3-C_6H_4
15	$P(OMe)_3$	3,5-$(CF_3)_2$-C_6H_3

Scheme 1

ligands of the starting material by the azadiene (**12**–**15**) or one CO and one phosphite are replaced to yield the (1-azadiene)Fe(CO)[$P(OMe)_3$]$_2$ complexes **9**–**11**.

As it was observed for $Fe(CO)_3$ complexes containing the same 1-azadiene ligands the NMR signals representing the hydrogen and carbon atoms of the azadiene chain in **1**–**15** are shifted highfield compared to the free ligands.[1] If there is an aromatic substituent at the imine nitrogen the resonances of the azadiene carbon and hydrogen atoms are of nearly the same value without any influence of the substituents at the aromatic system (**1**–**3**, **5**–**7**, **9**–**10**, **12**–**15**). If the substituent is a cyclohexyl group (**4**, **8**, **11**) the basicity of the imine nitrogen is increased and thus the hydrogen signals are slightly shifted to higher field. The carbon resonances of C2 are also observed at higher field compared to the analogous complexes with aromatic substituents whereas the signals of C1 and C3 are shifted downfield. The only exception is the resonance of C3 in **8** which is observed at $\delta = 68$.

As is expected the phosphine ligands also have an influence on the NMR spectroscopic properties of **1**–**15**. The most significant differences are observed for the carbon resonances representing C3 of the azadiene moieties. If the phosphine ligand is PPh_3 (**5**–**8**) those signals are observed at about $\delta = 67$. Using PCy_3 or $P(OMe)_3$, respectively, leads to a highfield shift of these resonances to $\delta = 59$ for complexes which exhibit an aromatic substituent at the imine nitrogen (**1**–**3**, **9**, **10**) atom and $\delta = 68$ for cyclohexyl substituted derivatives (**4**, **11**). The complexes with two $P(OMe)_3$ ligands (**12**–**15**) show all carbon resonances of the azadiene chain at higher field compared to their analogues with only one phosphine or phosphite ligand.

In the hydrogen NMR spectra the signals of H3 are the most sensitive ones with respect to variations of the phosphine or phosphite ligands. The PPh_3 derivatives (**5**–**8**) are observed in the most high field region, **1**–**4** with a PCy_3 ligand and **12**–**15** with two $P(OMe)_3$ ligands are found at nearly identical chemical shifts whereas the corresponding signals in **9**–**11**, which show only one phosphite group, are shifted to lower field.

Structural analysis

By recrystallization from mixtures of light petroleum and CH_2Cl_2 **1**–**5**, **7**–**13** and **15** were obtained as orange coloured crystals which were suitable for X-ray analyses. Fig. 1 shows the molecular structure of **1**, the numbering scheme

concerning the azadiene atoms which coordinate the iron center has been adopted for all other structure determinations. Selected bond lengths and angles are depicted in Table 1.

The coordination sphere around iron is a distorted square pyramid if the former azadiene C–C and C–N double bonds are considered to be the coordination sites. All compounds with just one phosphine or phosphite ligand due to steric reasons show this ligand in the axial position of the square pyramid.

The bond lengths observed for all compounds show some common features. The bond lengths of iron towards the two central carbon atoms of the azadiene chain (C1, C2) are nearly identical whereas Fe1–C3 is about 5–12 pm longer. Together with the shortening of the central carbon–carbon bond C1–C2 this again corresponds to the ligand to be described partly as a dianionic ligand with negative partial charges at N1 and C3 and a central double bond C1–C2 coordinating the iron atom *via* a coordinative bond like it was observed for the corresponding irontricarbonyl complexes with the same azadiene ligands.[1]

Table 2 summarizes the deviations of the atoms building up the azadiene chain from the plane through C1, C2, C3 and N1. For **1** the positions of the hydrogen atoms could not be detected from the difference Fourier map. The values for **12** are given as the average of two independent molecules which differ only very slightly concerning their bond lengths and angles.

(a)

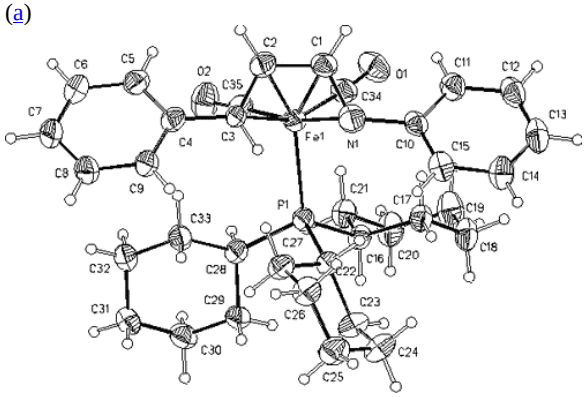

(b)

Fig. 1 (a) Molecular structure of **1**. (b) Click image or here to access 3D view of the structure.

Table 1 Selected bond lengths (pm) and angles (°) of **1**–**5**, **7**–**13** and **15**

Compound	Fe1–C1	Fe1–C2	Fe1–C3	Fe1–N1	C1–N1	C1–C2	C2–C3	Fe1–P1	Fe1–P2
1	205.1(5)	206.4(5)	216.6(4)	215.1(4)	139.7(7)	139.6(7)	135.5(6)	230.7(1)	—
2	206.2(7)	204.3(7)	217.8(6)	211.1(4)	137.1(8)	139.8(9)	140.1(9)	230.2(2)	—
3	207(1)	204(1)	219.0(8)	211.9(9)	139(1)	140(2)	140(1)	232.8(2)	—
4	209.5(2)	206.7(2)	218.5(2)	212.1(2)	135.2(3)	141.2(3)	142.2(3)	232.66(6)	—
5	205.7(5)	206.3(5)	217.0(5)	207.7(4)	136.3(7)	138.2(9)	140.7(8)	227.8(1)	—
7	207.4(3)	208.3(3)	217.9(3)	206.4(2)	136.1(4)	141.3(4)	141.3(4)	228.35(7)	—
8	206.8(2)	206.7(2)	218.4(1)	212.2(1)	135.6(2)	142.1(2)	142.5(2)	228.33(4)	—
9	205.9(3)	206.7(4)	213.8(4)	208.4(3)	137.8(5)	141.5(5)	142.7(5)	219.2(1)	—
10	207.7(7)	206.3(8)	211.4(7)	209.4(6)	135(1)	140(1)	144(1)	218.6(2)	—
11	208.3(4)	206.8(4)	216.8(4)	212.3(3)	135.8(5)	142.0(6)	142.1(6)	220.2(1)	—
12	204.9(5)	205.0(5)	215.3(6)	206.2(4)	134.7(7)	140.6(7)	142.0(8)	216.4(2)	216.4(2)
13	205.4(4)	206.0(4)	214.8(4)	207.5(3)	136.3(5)	140.1(6)	142.7(6)	216.5(1)	217.5(1)
15	208.9(2)	207.2(2)	215.5(2)	208.0(2)	137.0(3)	141.2(3)	143.3(3)	219.49(8)	218.01(9)

Compound	C10–N1–C1	N1–C1–C2	C1–C2–C3	C2–C3–C4	N1–Fe1–C1	C1–Fe1–C2	C2–Fe1–C3	N1–Fe1–C2	C1–Fe1–C3
1	121.3(4)	117.1(5)	117.0(5)	119.6(4)	38.8(2)	39.7(2)	37.3(2)	68.8(2)	67.5(2)
2	116.7(5)	115.5(6)	119.9(6)	123.3(5)	38.3(2)	39.8(3)	38.6(2)	68.6(2)	69.6(3)
3	115.7(9)	113.7(9)	120.5(7)	121.5(7)	38.6(3)	39.9(4)	38.6(4)	68.3(3)	69.7(4)
4	116.9(2)	116.7(2)	119.0(2)	121.4(2)	37.41(8)	39.66(9)	38.95(9)	68.35(8)	69.53(9)
5	119.2(5)	117.5(6)	118.3(6)	123.4(6)	38.5(2)	39.2(2)	38.7(2)	69.1(2)	68.9(2)
7	117.3(2)	116.4(2)	116.8(3)	124.5(2)	38.4(1)	39.7(1)	38.7(1)	69.3(1)	68.9(1)
8	113.4(1)	116.4(1)	116.3(1)	124.5(1)	37.73(6)	40.19(6)	39.06(6)	68.57(5)	69.21(6)
9	117.2(3)	115.7(3)	118.3(3)	123.1(3)	38.8(1)	40.1(1)	39.6(1)	69.5(1)	71.1(1)
10	118.4(6)	116.6(7)	116.7(8)	123.6(8)	37.6(3)	39.5(3)	40.2(3)	68.3(3)	70.3(3)
11	112.4(3)	116.1(4)	117.3(4)	123.4(4)	37.7(2)	40.0(2)	39.1(2)	68.5(1)	69.6(2)
12	122.0(5)	114.5(5)	116.3(5)	123.6(5)	38.2(2)	40.1(2)	39.4(2)	68.5(2)	69.6(2)
13	119.0(3)	115.8(3)	117.0(4)	124.4(4)	38.6(1)	39.8(2)	39.6(2)	69.0(1)	70.0(2)
15	120.6(2)	114.7(2)	117.3(2)	121.6(2)	38.37(9)	39.7(1)	39.6(1)	68.67(9)	69.8(1)

Table 2 Deviations (pm) from the plane (N1–C1–C2–C3) of **1**–**5**, **7**–**13** and **15**

Compound	N1	C1	H1	C2	H2	C3	H3
1	H1–3 could not be determined from difference Fourier map						
2	0.5	1.0	1.2	1.0	8.2	0.5	46.6
3	0.6	1.1	13.5	1.2	46.6	0.6	68.2
4	0.9	1.6	4.4	1.6	7.7	0.8	59.9
5	0.8	1.5	1.4	1.5	25.0	0.8	62.3
7	1.1	2.0	1.7	2.0	17.9	1.1	54.8
8	0.6	1.1	0.1	1.1	7.4	0.6	49.0
9	0.2	0.3	5.2	0.3	15.4	0.2	51.5
10	0.2	0.3	5.8	–0.3	18.7	0.2	73.0
11	0.5	1.0	5.8	1.0	14.9	0.5	57.7
12[a]	0.4	0.6	2.7	0.6	7.0	0.4	55.9
13	0.3	0.6	7.4	0.6	13.6	0.3	55.9
15	0.7	1.4	1.8	1.4	12.2	0.7	59.8

[a] The values given are the average of two independent molecules.

The position of H(C_3) is on average found 57.9 pm above the plane of the azadiene ligand. For derivatives of **1**–**15** with no phosphine or phosphite ligands present beneath the azadiene the corresponding proton was found 46.3 pm above the ligand's plane. So obviously the enhancement of electron density at the iron atoms induced by the phosphine ligands leads even more to the necessity to bend out H(C_3) in order to increase the overlap of molecular orbitals between the azadiene and the transition metal.

In order to analyze the arrangement of the complexes in the crystal lattices we normalized any C–H distance to 1.08 pm since it is well known that C–H distances found in X-ray crystallographic studies are too short compared with the distances observed in neutron scattering experiments, which are of higher accuracy. Only C–H···Y distances shorter than 270 pm were considered to be hydrogen bonds. All hydrogen atoms that are not involved in any hydrogen bonding were omitted for clarity in Figs. 2–13. Since the CF_3 groups in **3** and **7** are disordered C–H···F hydrogen bonds have not been analyzed although it has been pointed out recently that hydrogen bonding of that type might well contribute to a great extend to the stabilization of supramolecular structures.[5d] The different types of hydrogen bonds, their bond lengths and angles as well as the substructure built up by the specific hydrogen bond are summarized in Table 3.

Table 3 Hydrogen bond distances and angles in the crystal structures of **1**–**5**, **7**–**13** and **15**

Compound	C–H···Y hydrogen bond	H··Y (pm)	C–H···Y (deg)	C—Y (pm)	Substructure built up by hydrogen bond
1	C– H···O	261.9	123.0	333.3	Dimer
2	C–H···N	269.2	153.1	368.8	Chain
3	C–H···O	263.3	135.7	348.9	
	C–H···O	265.9	163.9	370.8	Chain
	C–H···O	261.6	134.0	345.4	Chain
	C–H···O	261.0	120.8	329.6	Chain
4	C–H···O	250.7	157.7	353.0	
	C–H···O	261.1	164.8	366.5	Dimer
	C–H···O	254.8	135.4	340.3	Dimer
5	—	—	—	—	—
7	C–H···O	251.0	128.1	328.8	Chain
	C–H···O	260.2	115.2	321.3	Dimer
8	C–H···O	259.3	131.7	340.9	Dimer
	C–H··$\pi_{C=C}$	261.5	147.3	357.2	Dimer
9	C–H···O	258.6	149.3	355.8	Chain
	C–H···O	266.2	134.0	350.0	Chain
	C–H···O	261.9	115.7	323.7	Chain
	C–H···O	263.7	143.8	356.6	Chain
10	C–H···O	269.5	138.1	357.3	Chain
	C–H···O	252.0	123.1	323.9	Chain
	C–H···O	267.7	164.8	373.0	Chain
11	C–H···O	246.5	150.6	344.7	Chain
	C–H···O	257.3	157.4	359.5	Chain
12	C–H···O	254.3	129.0	333.0	
	C–H···O	257.0	122.6	328.0	
	C–H···O	264.2	120.0	331.7	Dimer
	C–H···O	259.3	107.2	309.0	Chain
13	C–H···O	248.2	137.2	335.6	Dimer
	C–H···O	236.9	147.6	333.2	Chain
15	C–H···O	254.2	133.4	337.7	
	C–H···O	248.9	141.0	339.7	Dimer
	C–H···O	249.9	127.6	327.2	Chain

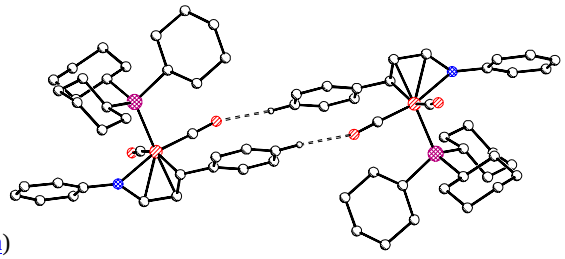

(a)

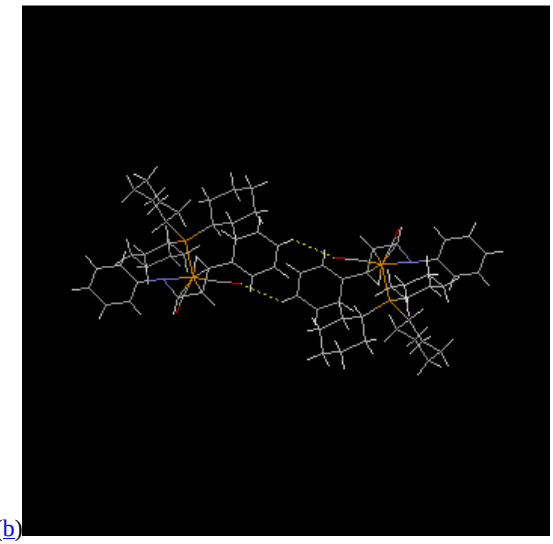

(b)

Fig. 2 (a) Crystal packing of **1**. Dimers are build up by two C–H···O interactions. (b) Click image or here to access 3D view of structure.

In most cases oxygen atoms of CO ligands or $P(OMe)_3$ groups act as hydrogen acceptors. But there are also two examples of hydrogen bonds of the C–H···N type (**2**, **9**) and one example of a hydrogen bond directed towards the centroid of an aromatic carbon carbon bond (**8**).

If one PPh_3 or PCy_3 ligand is present in the molecule there is one potential hydrogen bond acceptor site less compared to the (1-azadiene)$Fe(CO)_3$ complexes.[1] On the other hand, the number of groups being able to act as a hydrogen donor is higher as is the steric demand of the phosphine ligand compared to a CO group. If one CO in (1-azadiene)$Fe(CO)_3$ complexes is formally exchanged for one or two $P(OMe)_3$ ligands the number of hydrogen bond acceptor sites is increased. In addition, the methyl groups of $P(OMe)_3$ may also act as a hydrogen donor.

Fig. 2 shows the dimeric substructure built up in crystalline **1** by the interaction of an aromatic C–H function with a CO ligand of one neighboring molecule and *vice versa*. The hydrogen bonding network in the solid state structure of **2** consists of chains of molecules built up by interactions of the C–H···N type (Fig. 3). In crystalline **3** four C–H···O hydrogen bonds result in a 3D network with two different chain-like arrangements present. One of the chains is built up by two C–H–O interactions connecting the same neighboring molecules. Fig. 4 shows the arrangement built up by the combination of the two different chains. The structure gets even more complicated by a fourth C–H···O hydrogen bond connecting the infinite sheets shown in Fig. 4 by dimeric subunits. In the solid state of **4** two C–H···O hydrogen bonds build up a dimeric structure which, together with another dimer, leads to the formation of chains of dimers, which is depicted in Fig. 5.

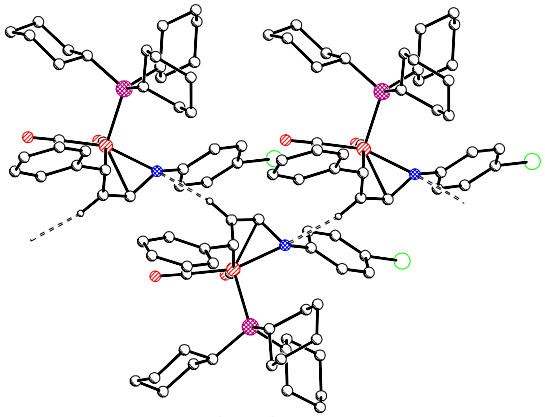

Fig. 3 Crystal packing of **2**. Infinite chains are built up by C–H···N interactions.

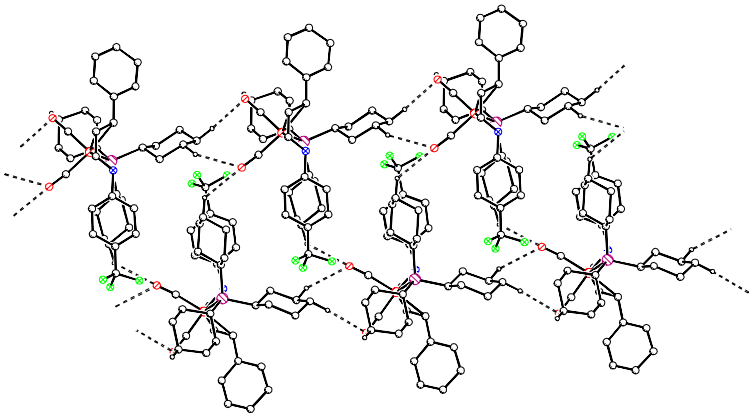

Fig. 4 Crystal packing of **3**. Two chain-like arrangements are produced by three different hydrogen bonds of the C–H···O type, combination of the chains results in a doubly strained packing pattern.

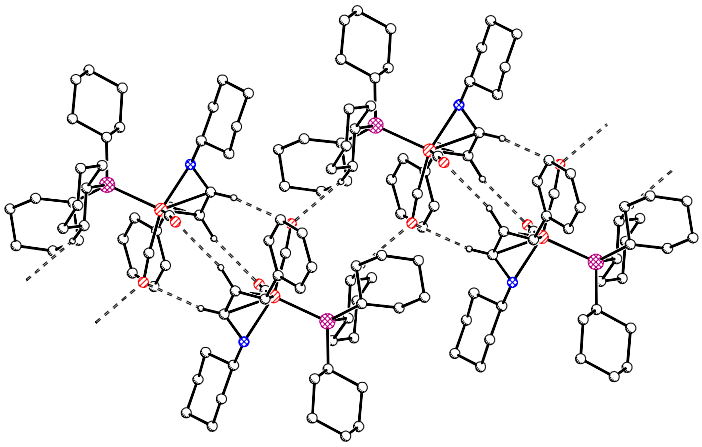

Fig. 5 Crystal packing of **4**. Two sorts of dimers are build up by three different C–H···O interactions and together form a chain of alternating dimeric substructures.

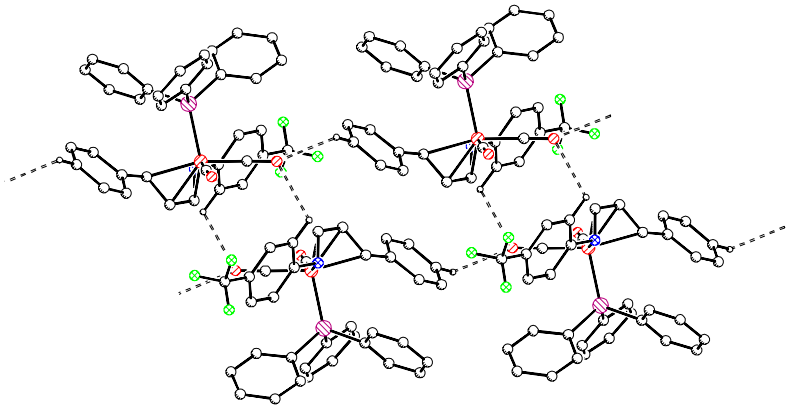

Fig. 6 Crystal packing of **7**. C–H···O interactions bring about the formation of dimers which are linked to chains by another C–H···O type of hydrogen bond.

The arrangement of molecules in the crystals of **7** which is shown in Fig. 6 is characterized by two interactions between CO ligands and C–H functions of the aromatic moieties of the azadiene ligands. One of these hydrogen bonds builds up chains of molecules whereas the other one brings about a dimeric substructure. As the result of a combination of both interactions a chain of dimers is formed with the PPh_3 ligands pointing towards outside the chain.

In contrast to the hydrogen bond system of **7** the solid state structure of **8** consists of two dimeric substructures which by combination result in the formation of a chain with alternating dimers similar to the one observed in the structure of **4** (Fig. 7). The crystals of **8** also are the only ones in which a hydrogen bond is made with the centroid of an aromatic carbon–carbon bond acting as the acceptor.

The use of $P(OMe)_3$ leads to an increase of potential hydrogen bond acceptor sites in the molecules. In addition, the high flexibility of those ligands makes the methyl groups highly effective hydrogen donor groups at the periphery of the complexes.

The solid state structure of **9** consists of a complicated network of hydrogen bonds built up by four different types

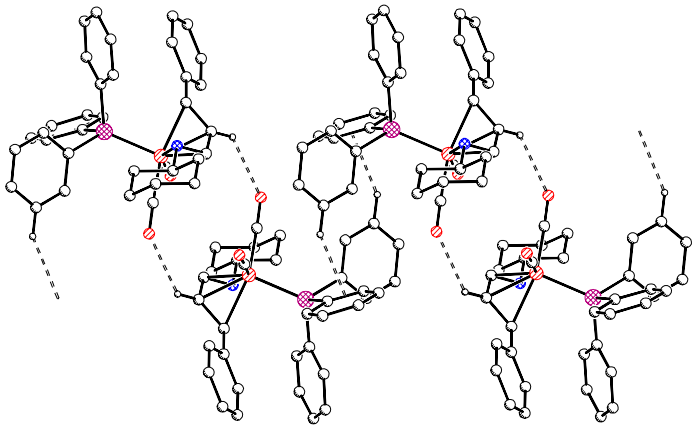

Fig. 7 Crystal packing of **8**. A chain of dimers is built up by one C–H···O and one C–H·$\pi_{C=C}$ interaction.

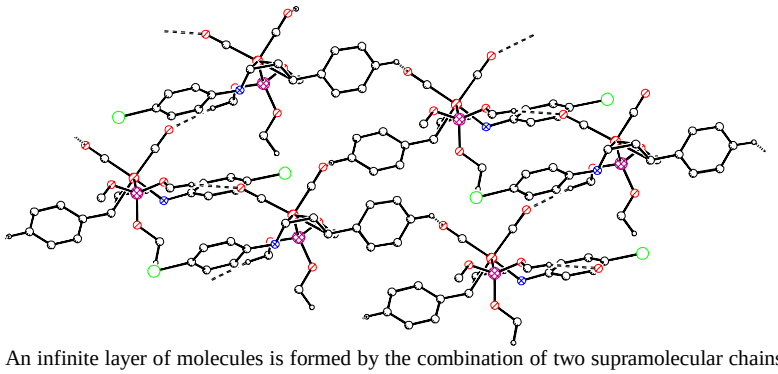

Fig. 8 Crystal packing of **9**. An infinite layer of molecules is formed by the combination of two supramolecular chains, two additional chain-like arrangements with longer hydrogen bond lengths are not shown for the sake of clarity, but result in the formation of an infinite 3D network.

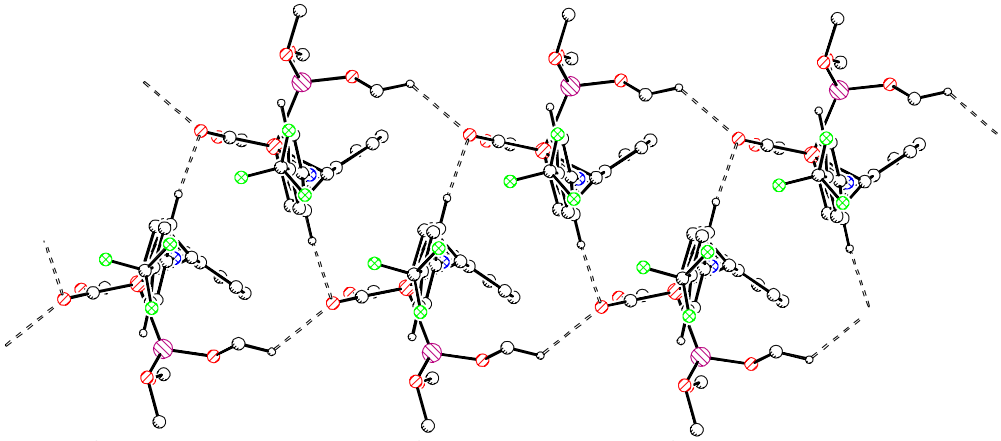

Fig. 9 Crystal packing of **10**. A double chain arrangement is formed by the combination of two chains created by C–H···O interactions, a third chain of C–H···O hydrogen bonds again connects the chains of complexes to 3D infinite networks.

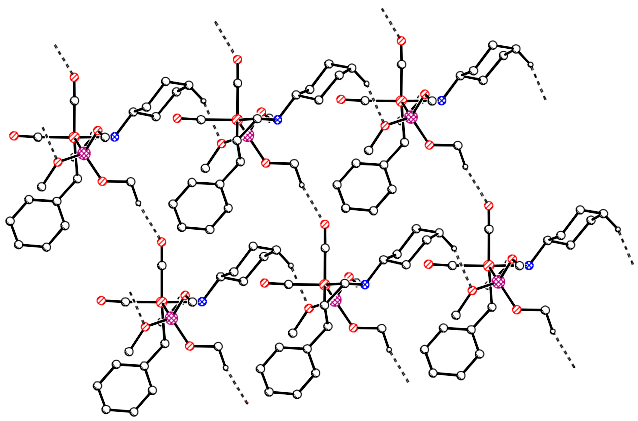

Fig. 10 Crystal packing of **11**. Two different types of chains built up by C–H···O interactions together form an infinite network.

of chains. Like in the crystals of **2** with a PCy_3 ligand instead of the phosphite in **9** there also is a C–H···N interaction between the imine nitrogen and one of the hydrogen atoms at the azadiene moiety. In contrast to **2** there is one C–H···O hydrogen bond between a CO ligand and one of the aromatic rings of the azadiene ligand present. These two chains are linked by further C–H···O contacts between the CO ligands and hydrogen atoms belonging to the methyl groups of the $P(OMe)_3$ ligands. The oxygen atoms of the phosphites are not involved in the hydrogen bonding system. Fig. 8 shows the combination of those two chain-like arrangements in the solid state structure of **9** which show the shortest C–H···O contacts.

The packing of molecules in **10** is also composed of two different chains brought about by hydrogen bonds of the C–H···O type between CO groups and hydrogen atoms of the aromatic substituents of the azadiene ligand. Again this combination of chains that is similar to the one observed for **3** is connected to 3D networks by additional hydrogen bonds between one of the CO ligands and the methyl group of the $P(OMe)_3$. Fig. 9 shows the doubly strained arrangement which is brought about by the two hydrogen bonds with the shortest C–H···O contacts.

The structure of **11** shows the presence of one C–H···O interaction between an oxygen atom of the phosphite group

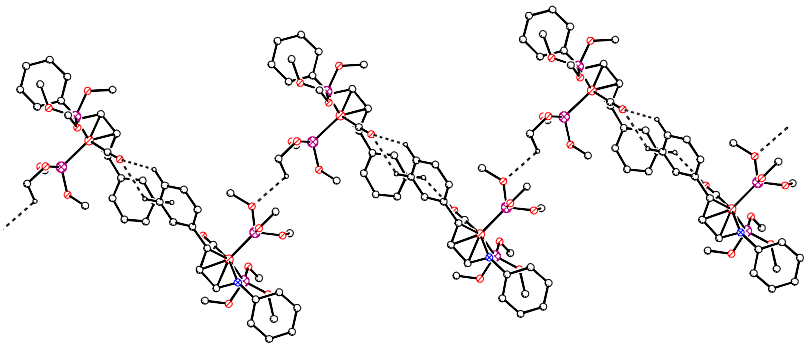

Fig. 11 Crystal packing of **12**. Dimers built up by two different hydrogen bonds of the C–H···O type are linked to chains of dimers by an additional C–H···O interaction.

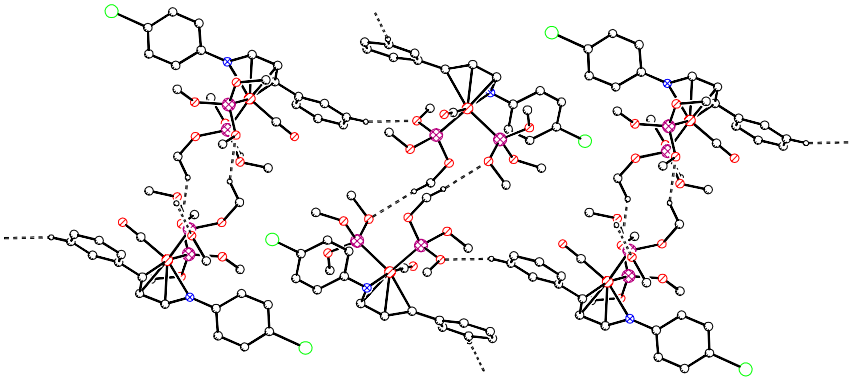

Fig. 12 Crystal packing of **13**. Chains of dimers are formed by two types of C–H···O interactions.

and a C–H function of one of the groups of the azadiene ligand. The chains formed by this hydrogen bonds are connected to a double chain shown in Fig. 10 by additional hydrogen bonds between one CO ligand and the hydrogen atom of one of the methyl groups. So the structure of **11** is the only one observed in this work which is only built up by hydrogen bonds using the $P(OMe)_3$ ligand either as the donor or acceptor of hydrogen bonds whereas all the other structures at least involve the CO ligands as hydrogen bond accepting groups.

In the complexes **12**–**15** there are two $P(OMe)_3$ ligands beneath the azadiene and one terminal CO. So one should expect the crystal structures to show hydrogen bond networks mainly built up by interactions involving the phosphite ligands either as acceptor or donor sites of intermolecular hydrogen bonding.

The crystal structure of **12** consists of two symmetry independent molecules and the arrangement of the molecules is shown in Fig. 11. It is brought about by the formation of dimers in which the two independent molecules are linked by three intermolecular hydrogen bonds all involving the remaining CO ligand as the acceptor site. The CO ligand of one molecule builds up a bifurcated hydrogen bond towards two aromatic protons of a phenyl substituent belonging to the neighboring molecule. The CO group of the second molecule also interacts with one aromatic proton of the azadiene of the first complex. Those dimers are linked to chains of dimers by a hydrogen bond between the two phosphite ligands in apical position of neighboring molecules. The second phosphite ligand adopting an equatorial position in the complexes is not involved in any hydrogen bonding in the crystal structure of **12**.

The crystal structure of **13** is quite similar to the one of **12**. It also consists of chains of dimers and is shown in Fig. 12. The dimers now are constructed by hydrogen bonding between the two phosphite ligands in a way that the $P(OMe)_3$ moiety in the apical position of one complex interacts with the equatorial phosphite of a neighboring molecule and *vice versa*. These dimers are connected to form chains of dimers by the interaction between one oxygen atom of the apical phosphite and a phenyl group of the next dimer. So in this crystal structure the CO ligand is not involved in any hydrogen bonding.

The hydrogen bonding in the crystal structure of **15** as **12** and **13** shows chains of dimers but again the construction of this motive is different to the ones before (Fig. 13). The dimers are brought about by hydrogen bonds between the CO ligands and hydrogen atoms of the azadiene of the next molecule. These dimers now are linked to form chains by interactions between the equatorial phosphite ligands of neighboring molecules in which two oxygen and two hydrogen atoms of the same ligand form a total of four hydrogen bonds to the corresponding phosphite of the neighboring complex.

Conclusions

The research reported herein was motivated by two objectives. The first one was the question whether the formal substitution of one or more CO ligands in (1-azadiene)$Fe(CO)_3$ complexes by various phosphorus containing ligands makes it possible to tune the properties of the C–H bond in β-position with respect to the imine double bond. We were interested in this point since this specific C–H bond is activated in the course of several

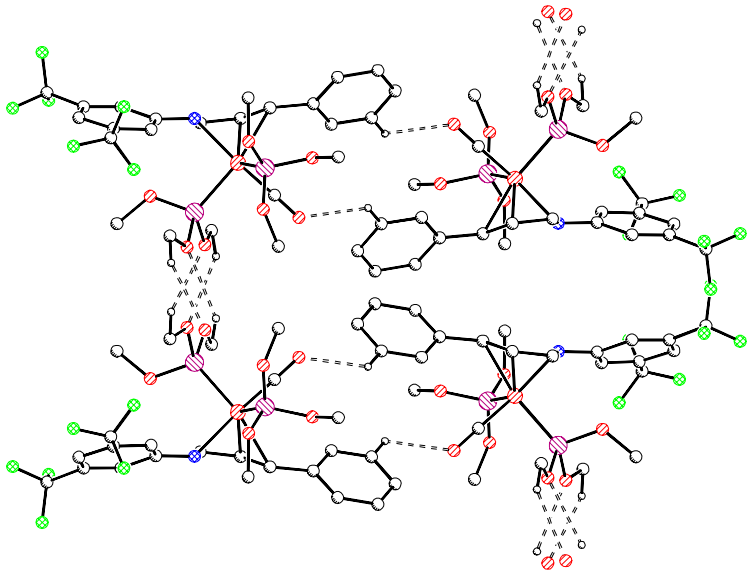

Fig. 13 Crystal packing of **15**. A chain of dimers is built up by three different hydrogen bonds of the C–H···O type.

Table 4 Crystal and intensity data for the compounds **1**–**5**, **7** and **8**

	1	**2**	**3**	**4**	**5**	**7**	**8**
Formula	$C_{35}H_{46}FeNO_2P$	$C_{35}H_{45}BrFeNO_2P \cdot Et_2O$	$C_{36}H_{45}F_3FeNO_2P$	$C_{35}H_{52}FeNO_2P$	$C_{35}H_{28}FeNO_2P \cdot 0.2$ THF	$C_{36}H_{27}F_3NO_2P$	$C_{35}H_{34}FeNO_2P$
Molecular weight/g mol^{-1}	599.55	752.57	667.55	605.60	595.82	649.41	587.45
Temperature/K	293	183	183	183	183	183	183
a/Å	10.656(2)	11.9029(8)	11.167(2)	10.7936(4)	15.591(2)	10.0660(3)	10.6186(3)
b/Å	11.120(2)	32.675(3)	10.538(2)	18.0338(7)	12.6381(9)	11.6131(5)	12.1183(3)
c/Å	14.733(3)	9.672(1)	28.738(2)	16.5783(4)	16.937(2)	14.4800(6)	13.9154(2)
α/°	90.87(1)	90	90	90	90	67.253(2)	65.317(1)
β/°	104.266(9)	97.22(6)	100.288(7)	95.974(3)	99.046(4)	81.850(3)	84.427(1)
γ/°	110.03(1)	90	90	90	90	86.625(3)	68.745(1)
V/Å^3	1580.1(6)	3731.7(6)	3327.4(7)	3209.4(2)	3295.8(5)	1545.2(1)	1513.23(6)
Z	2	4	4	4	4	2	2
Crystal system	Triclinic	Monoclinic	Monoclinic	Monoclinic	Monoclinic	Triclinic	Triclinic
Space group	$P\bar{1}$	$P2_1/c$	$P2_1/c$	$P2_1/n$	$P2_1/n$	$P\bar{1}$	$P\bar{1}$
Absorption coefficient/mm^{-1}	0.560	1.554	0.552	0.552	0.537	0.591	0.583
Reflections measured	4152	5922	4422	8538	8469	4138	6108
Independent reflections	4152	3449	2535	4519	4568	4138	6108
R_{int}	—	0.0496	0.1250	0.0340	0.0525	—	—
Reflections observed [$F_o^2 > 2\sigma(F_o^2)$]	3442	2789	1763	3873	3188	3765	5530
No. of parameters	373	432	422	378	420	466	497
R_1	0.0584	0.0491	0.0794	0.0307	0.0560	0.0430	0.0288
wR_2	0.1512	0.1265	0.1724	0.0878	0.1464	0.1109	0.0714

catalytic C–C coupling reactions using $Ru_3(CO)_{12}$ as the precatalyst. We found that the out of plane position of this hydrogen atom with respect to the C–C–C–N plane of the azadiene ligand is on average increased by about 10 pm for the phosphine or phosphite complexes that we were able to characterize structurally compared to their iron tricarbonyl derivatives. This out of plane position is necessary in order to increase the overlap of molecular orbitals between the azadiene and the transition metal. So the increased electron density at the iron atom induced by formally substituting a CO against a phosphine or phosphite, respectively, obviously weakened the carbon iron bond and thus made it necessary for the ligand to shift the corresponding hydrogen atom even more out of the plane of the ligand in order to stabilize the complexes.

The second question that arose was whether it is possible to induce distinct changes in the supramolecular arrangement of molecules in the crystals by the variation of ligands. The formal substitution of CO with a phosphine or phosphite not only changes the steric demands of the complexes but also changes the number and nature of potential hydrogen bond acceptor or donor sites and thus may have a distinct influence on the crystal properties. First we found that for all complexes with just one phosphorus containing ligand this ligand adopts the apical position in the square pyramidal coordination sphere of the iron atom. The use of PCy_3 or PPh_3 mostly leads to the formation of dimers or chains by hydrogen bonding between the remaining CO ligands and C–H bonds, either of the organic substituents of the azadiene or suitable C–H bonds of the organic moieties at the phosphine ligands. The hydrophobic phenyl or cyclohexyl groups point towards the outside of these dimers or chains, respectively.

The use of one $P(OMe)_3$ leads to similar substructures which are now linked by additional hydrogen bonds involving both oxygen and hydrogen atoms of the phosphite ligands as hydrogen bond acceptor or donor sites. So the resulting hydrogen bond systems are much more

complicated than for the PPh_3 or PCy_3 derivatives. If two $P(OMe)_3$ ligands are present in the molecule the steric effect of these rather large ligands again leads to a simplification of the supramolecular architecture of the organometallic crystals, which now in these cases occur as chains of dimers.

Experimental

General

All procedures were carried out under an argon atmosphere in anhydrous, freshly distilled solvents. Chromatography was done using silica gel 60 and silanized silica gel 60, 70–230 mesh ASTM (Merck), which were dried at 10^{-2} bar (10^3 Pa) for 2 d before use. The mononuclear starting compounds were prepared from irradiation of $Fe(CO)_5$ with the corresponding imine following a literature procedure.[7] Infrared spectra were recorded on a Perkin Elmer FT-IR System 2000 using 0.2 mm KBr cuvettes. NMR spectra were recorded on a Bruker AC 200 spectrometer (^{1}H: 200 MHz with $SiMe_4$ as internal standard, ^{13}C: 50.32 MHz with $CDCl_3$ as internal standard; ^{31}P: 81.03 MHz with 85% D_3PO_4 as external standard). Mass spectra were recorded on a Finnigan MAT SSQ 710 instrument. High resolution mass spectrometry (HRMS) was done using a Finnigan MAT 95 XL instrument with ESI techniques and methanol as the solvent. Elemental analyses were carried out at the laboratory of the Institute of Organic Chemistry and Macromolecular Chemistry of the Friedrich-Schiller-University Jena.

X-Ray crystallographic study

Structure determination of **12** was carried out on a Siemens P4 diffractometer. Structure determinations of **1**–**5**, **7**–**11**, **13** and **15** were carried out using an Enraf Nonius Kappa CCD diffractometer, crystal detector distance 25 mm, 180 frames. In both cases graphite monochromated Mo-Kα radiation was used. The crystals were mounted in a stream of cold nitrogen. Data were corrected for Lorentz and polarization effects but not for absorption. The structures were solved by direct methods and refined by full-matrix least squares techniques against F^2 using the programs SHELXS86 and SHELXL93.[8] Computations of the structures were done with the program XPMA and the molecular illustrations were drawn using the program XP.[9,10] The crystal and intensity data are given in Table 4 and Table 5. Click here for full crystallographic data (CCDC number 1350/10).

Preparation of the compounds. In a typical experiment 1 mmol of the mononuclear starting complex [$Fe(CO)_4(PCy_3)$: 448 mg, $Fe(CO)_4(PPh_3)$: 430 mg, $Fe(CO)_3(P(OMe)_3)_2$: 388 mg] are irradiated for 4 h with a 1.5 excess of the corresponding azadiene ligand. Every half an hour argon is bubbled through the solution for 5 min to remove CO which is set free during the reaction. After the reaction is finished the volatile components are evaporated *in vacuo*. The crude reaction product is dissolved in 5 ml CH_2Cl_2, 1 g silanized silica gel is added and the solvent again is removed *in vacuo*. Purification of the compounds is then achieved by column chromatography under inert conditions. Most of the products may be obtained as an orange coloured zone by using a mixture of light petroleum (bp 40–60 °C) and diethyl ether (10 : 1 or 5 : 1) as the eluent. If the polarities of the starting complex and the product are very similar purification may only be achieved by subsequent crystallization. If $Fe(CO)_3[P(OMe)_3]_2$ is used as the starting compound either two CO ligands are substituted by the azadiene ligand or one CO and one $P(OMe)_3$ moiety are replaced by the azadiene, respectively. During the chromatographic work-up the product complex with one $P(OMe)_3$ ligand is always obtained with mixtures containing a smaller amount of ether.

All compounds may be recrystallized from mixtures of light petroleum–CH_2Cl_2 at –20 °C to give orange coloured crystals.

MS and spectroscopic data of 1. MS (EI): *m/z* (%) 543 (M^+ – 2 CO, 10), 336 ($C_{18}H_{33}PFe^+$, 2), 280 (PCy_3^+, 6), 263 ($C_{15}H_{13}NFe^+$, 30), 206 ($C_{15}H_{12}N^+$, 100), 198 ($C_{12}H_{23}P^+$, 10), 117 ($C_6H_{14}P^+$, 19), 77 ($C_6H_5^+$, 26); IR (cm^{-1}) (CH_2Cl_2, 298 K): 1977 vs, 1925 vs; ^{1}H NMR (ppm) ($CDCl_3$, 298 K):

Table 5 Crystal and intensity data for the compounds **9**–**13** and **15**

	9	**10**	**11**	**12**	**13**	**15**
Formula	$C_{20}H_{21}BrFeNO_5P$	$C_{21}H_{21}F_3FeNO_5P$	$C_{20}H_{28}FeNO_5P$	$C_{22}H_{31}FeNO_7P_2$	$C_{22}H_{30}BrFeNO_7P_2$	$C_{24}H_{29}F_6NO_7P_2$
Molecular weight/g mol^{-1}	522.11	511.21	449.25	539.27	618.17	675.27
Temperature/K	183	183	183	213	183	183
a/Å	9.9843(6)	16.416(2)	14.9615(5)	12.561(3)	13.285(1)	22.0475(4)
b/Å	7.8002(4)	16.848(2)	16.6780(7)	14.316(4)	16.678(1)	15.4116(5)
c/Å	14.1502(7)	8.3990(9)	8.9100(4)	14.258(3)	11.8678(9)	8.5368(2)
α/°	90	90	90	90	90	90
β/°	96.99(3)	98.616(6)	101.902(4)	101.31(1)	98.368(6)	90.977(2)
γ/°	90	90	90	90	90	90
V/Å^3	1093.8(1)	2296.7(4)	2175.5(2)	2514(1)	2601.6(4)	2900.3(1)
Z	2	4	4	4	4	2
Crystal system	Monoclinic	Monoclinic	Monoclinic	Monoclinic	Monoclinic	Monoclinic
Space group	$P2_1$	*Cc*	*Cc*	$P2_1$	$P2_1/c$	$P2_1/c$
Absorption coefficient/mm^{-1}	2.619	0.782	0.796	0.770	2.280	0.712
Reflections measured	8741	1113	2907	7330	6697	5880
Independent reflections	4492	1113	1621	6602	3620	5880
R_{int}	0.0394	—	0.0277	0.0495	0.0393	—
Reflections observed [$F_o^2 > 2\sigma(F_o^2)$]	4006	1063	1568	5097	3192	4869
No. of parameters	279	307	333	631	374	486
R_1	0.0364	0.0383	0.0238	0.0466	0.0377	0.0406
wR_2	0.0801	0.0914	0.0664	0.0975	0.0996	0.0991

1.11–2.18 (m, 33H), 2.44–2.53 (m, 1H), 5.30–5.35 (m, 1H), 6.90 (m, 1H), 7.06–7.27 (m, 10H); ^{13}C NMR (ppm) ($CDCl_3$, 298 K): 26.3, 27.6, 27.7 (d, $^2J_{PC}$ = 9.8 Hz), 29.1 (d, $^3J_{PC}$ = 16.5 Hz), 36.5 (d, $^1J_{PC}$=16.0 Hz), 59.3, 77.2, 101.1, 122.4, 123.3, 124.7, 126.6, 128.3, 142.7, 154.1, 211.8, 215.0; ^{31}P NMR (ppm) ($CDCl_3$, 298 K): 50.9.

MS and spectroscopic data of 2. MS (EI): *m/z* (%) 623 (M^+ – 2 CO, 2), 364 ($Fe(CO)PCy_3^+$, 46), 343 ($C_{15}H_{12}NBrFe^+$, 1), 336 ($FePCy_3^+$, 13), 286 ($C_{15}H_{11}NBr^+$, 13), 280 (PCy_3^+, 97), 198 ($C_{12}H_{23}P^+$, 100), 115 ($C_6H_{12}P^+$, 53); IR (cm^{-1}) (CH_2Cl_2, 298 K): 1971 vs, 1906 vs; ^{1}H NMR (ppm) ($CDCl_3$, 298 K): 1.03–1.95 (m, 30H), 2.18–2.21 (m, 3H), 2.45–2.50 (m, 1H), 5.32–5.35 (m, 1H), 6.78 (m, 1H), 6.91–6.93 (m, 2H), 7.05–7.09 (m, 1H), 7.18–7.25 (m, 6H); ^{13}C NMR (ppm) ($CDCl_3$, 298 K): 26.3, 27.5 (br), 29.0 (d, $^3J_{PC}$ = 33.0 Hz), 36.4 (d, $^1J_{PC}$ = 15.9 Hz), 59.9, 77.2, 99.7, 114.7, 124.7, 124.8, 126.6, 128.3, 134.3, 142.3, 153.4, 211.5, 215.5; ^{31}P NMR (ppm) ($CDCl_3$, 298 K): 51.0.

MS and spectroscopic data of 3. MS (EI): *m/z* (%) 667 (M^+, 2), 611 (M^+ – 2 CO, 30), 331 ($C_{16}H_{12}F_3NFe^+$, 10), 280 (PCy_3^+, 23), 274 ($C_{16}H_{11}F_3N^+$, 83), 198 ($C_{12}H_{23}P^+$, 80), 117 ($C_6H_{14}P^+$, 100); IR (cm^{-1}) (CH_2Cl_2, 298 K): 1974 vs, 1926 vs; ^{1}H NMR (ppm) ($CDCl_3$, 298 K): 1.15–2.24 (m, 33H), 2.55–2.57 (m, 1H), 5.37–5.41 (m, 1H), 6.77 (m, 1H), 7.03–7.40 (m, 9H); ^{13}C NMR (ppm) ($CDCl_3$, 298 K): 26.1, 27.6 (br), 29.3, 36.6 (d, $^1J_{PC}$ = 15.5 Hz), 60.5, 78.0, 98.6, 122.8, 126.6, 127.1 (q, $^1J_{CF}$ = 270.0 Hz), 127.5, 128.4, 128.8, 142.1, 157.8, no CO resonances have been observed; ^{31}P NMR (ppm) ($CDCl_3$, 298 K): 51.4.

MS and spectroscopic data of 4. MS (EI): *m/z* (%) 605 (M^+ – 2 CO, 1), 577 (M^+ – CO, 1), 364 ($Fe(CO)(PCy_3)^+$, 29), 297 ($C_{15}H_{19}NFe(CO)^+$, 11), 280 (PCy_3^+, 35), 269 ($C_{15}H_{19}NFe^+$, 58), 213 ($C_{15}H_{19}N^+$, 68), 198 ($C_{12}H_{23}P^+$, 83), 115 ($C_6H_{12}P^+$, 100); IR (cm^{-1}) (CH_2Cl_2, 298 K): 1925 vs; ^{1}H NMR (ppm) ($CDCl_3$, 298 K): 1.14–2.24 (m, 45H), 5.03–5.07 (m, 1H), 6.48 (m, 1H), 7.13–7.21 (m, 5H); ^{13}C NMR (ppm) ($CDCl_3$, 298 K): 24.4, 25.3, 35.8, 36.3, 37.4, 60.5, 66.7, 71.5, 110.7, 126.1, 128.1, 128.5, 139.4, no CO resonances have been observed; ^{31}P NMR (ppm) ($CDCl_3$, 298 K): 52.2.

MS and spectroscopic data of 5. MS (EI): *m/z* (%) 581 (M^+, 1), 525 (M^+ – 2 CO, 7), 318 (Ph_3PFe^+, 25), 263 ($C_{15}H_{13}NFe^+$, 92), 262 (Ph_3P^+, 56), 206 ($C_{15}H_{12}N^+$, 100), 183 ($C_{12}H_8P^+$, 28), 108 (PhP^+, 27); IR (cm^{-1}) (CH_2Cl_2, 298 K): 1981 vs, 1924 vs; ^{1}H NMR (ppm) ($CDCl_3$, 298 K): 2.03–2.12 (m, 1H), 5.56–5.61 (m, 1H), 6.40–6.43 (m, 2H), 6.68–6.72 (m, 1H), 6.80 (m, 1H), 7.08–7.40 (m, 22H); ^{13}C-NMR (ppm) ($CDCl_3$, 298 K): 66.2, 77.9, 101.7, 120.5, 121.8, 125.3, 126.0, 129.8, 128.4 (br), 133.2, 133.5 (br), 134.5 (d, $^1J_{PC}$ = 37.8 Hz), 141.2, 156.3, no CO resonances have been observed; ^{31}P NMR (ppm) ($CDCl_3$, 298 K): 49.9.

MS and spectroscopic data of 6. MS (EI): *m/z* (%) 605 (M^+ – 2 CO, 2), 318 (Ph_3PFe^+, 19), 284 ($C_{15}H_{11}NBr^+$, 31), 262 (Ph_3P^+, 100), 183 ($C_{12}H_8P^+$, 71), 108 (PhP^+, 36); IR (cm^{-1}) (CH_2Cl_2, 298 K): 1980 vs, 1929 vs; ^{1}H NMR (ppm) ($CDCl_3$, 298 K): 2.07 (m, 1H), 5.59 (m, 1H), 6.38–6.43 (m, 2H), 6.56 (m, 4H), 6.70 (m, 1H), 7.05–7.14 (m, 8H), 7.24–7.42 (m, 10H); ^{13}C NMR (ppm) ($CDCl_3$, 298 K): 66.5, 78.4, 100.7, 112.8, 123.3, 125.5, 126.0, 128.4 (d, $^2J_{PC}$ = 9.4 Hz), 128.5, 130.0 (d, $^4J_{PC}$ = 2.0 Hz), 131.2, 133.5 (d, $^3J_{PC}$=10.6 Hz), 134.3 (d, $^1J_{PC}$ = 38.5 Hz), 141.0, 154.4, 209.9, 212.7, 212.9; ^{31}P NMR (ppm) ($CDCl_3$, 298 K): 49.4.

MS and spectroscopic data of 7. MS (EI): *m/z* (%) 649 (M^+, 1), 621 (M^+ – CO, 1), 593 (M^+ – 2 CO, 15), 331 ($C_{16}H_{12}F_3NFe^+$, 48), 275 ($C_{16}H_{12}F_3N^+$, 1), 262 (Ph_3P^+, 100), 183 ($C_{12}H_8P^+$, 65), 108 (PhP^+, 36); IR (cm^{-1}) (CH_2Cl_2, 298 K): 1989 vs, 1933 vs; ^{1}H NMR (ppm) ($CDCl_3$, 298 K): 2.12–2.17 (m, 1H), 5.61–5.66 (m, 1H), 6.39–6.43 (m, 4H), 6.70 (m, 1H), 6.90–7.13 (m, 20H); ^{13}C NMR (ppm) ($CDCl_3$, 298 K): 66.8, 79.1, 99.5, 121.5, 122.2, 125.5, 125.6, 126.1, 128.5 (d, $^2J_{PC}$ = 9.0 Hz), 130.1 (d, $^4J_{PC}$ = 2.0 Hz), 133.6 (d, $^3J_{PC}$ = 10.5 Hz), 134.2 (d, $^1J_{PC}$ = 38.7 Hz), 140.8, 158.5, 209.6, 212.6, 212.8, the expected quartets representing the CF_3 group and the aromatic carbon atom attached to it were not observed; ^{31}P NMR (ppm) ($CDCl_3$, 298 K): 49.6.

MS and spectroscopic data of 8. MS (EI): *m/z* (%) 587 (M^+, 2), 559 (M^+ – CO, 7), 531 (M^+ – 2 CO, 86), 318 (Ph_3PFe^+, 3), 269 ($C_{15}H_{19}NFe^+$, 100), 262 (Ph_3P^+, 65), 213 ($C_{12}H_8P^+$, 47), 183 ($C_{12}H_8P^+$, 47), 108 (PhP^+, 22); IR (cm^{-1}) (CH_2Cl_2, 298 K): 1971 vs, 1914 vs; ^{1}H NMR (ppm) ($CDCl_3$, 298 K): 0.67–0.75 (m, 4H), 1.07–1.39 (m, 5H), 1.63–1.81 (m, 3H), 1.85–1.90 (m, 1H), 5.36–5.39 (m, 1H), 6.32–6.46 (m, 2H), 6.46 (m, 1H), 6.99–7.35 (m, 18H); ^{13}C NMR (ppm) ($CDCl_3$, 298 K): 25.5, 25.6, 25.7, 35.9, 38.3, 65.2, 68.1, 74.8, 109.2, 124.9, 125.7, 128.0 (d, $^2J_{PC}$ = 22.4 Hz), 128.3, 129.5 (d, $^4J_{PC}$ = 1.6 Hz), 133.5 (d, $^3J_{PC}$ = 10.4 Hz), 135.5 (d, $^1J_{PC}$ = 37.1 Hz), 141.7, 211.7, 213.4; ^{31}P NMR (ppm) ($CDCl_3$, 298 K): 47.6.

MS and spectroscopic data of 9. MS (EI): *m/z* (%) 521 (M^+, 6), 493 (M^+ – CO, 11), 465 (M^+ – 2 CO, 48), 341 ($C_{15}H_{12}NBrFe^+$, 100), 284 ($C_{15}H_{11}NBr^+$, 33), 93 ($P(OMe)_2^+$, 94); IR (cm^{-1}) (CH_2Cl_2, 298 K): 1998 vs, 1944 vs; ^{1}H NMR (ppm) ($CDCl_3$, 298 K): 2.70–2.85 (m, 1H), 3.61 (d, 9H, $^3J_{PH}$ = 10.9 Hz), 5.46–5.54 (m, 1H), 6.61 (m, 1H), 6.78–6.83 (m, 4H), 7.09–7.20 (m, 5H); ^{13}C NMR (ppm) ($CDCl_3$, 298 K): 51.9 (d, $^2J_{PC}$ = 4.9 Hz), 58.7, 75.2, 100.0, 113.3, 123.4, 125.6, 126.7, 128.3, 131.5, 141.0, 154.5, no CO resonances have been observed; ^{31}P NMR (ppm) ($CDCl_3$, 298 K): 175.5.

MS and spectroscopic data of 10. MS (EI): *m/z* (%) 511 (M^+, 6), 483 (M^+ – CO, 6), 387 ($C_{18}H_{12}F_3NO_2Fe^+$, 7), 275 ($C_{16}H_{12}F_3N^+$, 100); IR (cm^{-1}) (CH_2Cl_2, 298 K): 1998 vs, 1942 vs; ^{1}H NMR (ppm) ($CDCl_3$, 298 K): 2.77 (m, 1H), 3.61 (d, 9H, $^3J_{PH}$ = 10.7 Hz), 5.51 (m, 1H), 6.59 (m, 1H), 6.92–7.37 (m, 4H), 7.10–7.30 (m, 5H); ^{13}C NMR (ppm) ($CDCl_3$, 298 K): 51.9 (d, $^2J_{PC}$ = 4.7 Hz), 58.7, 76.6, 98.8, 121.4, 122.2 (q, $^2J_{CF}$ = 33.0 Hz), 124.7 (q, $^1J_{CF}$ = 271.2 Hz), 125.7, 125.8, 126.5, 128.3, 140.8, 158.5, 208.0, 212.2; ^{31}P NMR (ppm) ($CDCl_3$, 298 K): 175.4.

MS and spectroscopic data of 11. MS (EI): *m/z* (%) 449 (M^+, 1), 421 (M^+ – CO, 3), 393 (M^+ – 2 CO, 9), 269 ($C_{15}H_{19}NFe^+$, 100); IR (cm^{-1}) (CH_2Cl_2, 298 K): 1988 vs, 1917 vs; ^{1}H NMR (ppm) ($CDCl_3$, 298 K): 0.86–2.05 (m, 11H), 2.49 (m, 1H), 3.25 (d, 9H, $^3J_{PH}$ = 9.9 Hz), 4.96 (m, 1H), 5.96 (m, 1H), 6.88–7.14 (m, 5H); ^{13}C NMR (ppm) ($CDCl_3$, 298 K): 25.5, 25.9, 35.6, 38.2, 51.7 (br), 52.6, 67.7, 72.7, 108.3, 125.1, 126.7, 127.9, 141.6, 210.7, 211.5; ^{31}P NMR (ppm) ($CDCl_3$, 298 K): 178.3.

MS and spectroscopic data of 12. MS (EI): *m/z* (%) 539 (M^+, 3), 511 (M^+ – CO, 1), 263 ($C_{15}H_{13}NFe^+$, 100), 206 ($C_{15}H_{12}N^+$, 17), 124 ($P(OMe)_3^+$, 8), 93 ($P(OMe)_2^+$, 36); IR (cm^{-1}) (CH_2Cl_2, 298 K): 1925 vs; ^{1}H NMR (ppm) ($CDCl_3$, 298 K): 2.45 (m, 1H), 3.32 (d, 9H, $^3J_{HP}$ = 10.9 Hz), 3.59 (d, 9H, $^3J_{HP}$ = 10.9 Hz), 5.18–5.22 (m, 1H), 6.46 (m, 1H), 6.93–7.32 (m, 10H); ^{13}C NMR (ppm) ($CDCl_3$, 298 K): 51.3

(br), 52.8, 53.2, 73.5, 96.8, 118.7, 121.3, 124.2, 126.6, 127.0, 127.9, 143.3, 154.8, 215.0; ^{31}P NMR (ppm) ($CDCl_3$, 298 K): 172.7, 181.7.

MS and spectroscopic data of 13. MS (EI): *m/z* (%) 617 (M^+, 3), 599 (M^+ – CO, 1), 467 ($C_{18}H_{21}BrNO_3PFe^+$, 12), 341 ($C_{15}H_{12}BrNFe^+$, 12), 286 ($C_{15}H_{11}BrN^+$, 100), 204 ($C_{15}H_{10}N^+$, 30), 124 $(P(OMe)_3)^+$, 18), 93 $(P(OMe)_2)^+$, 56), 81 (Br^+, 18), 63 (CH_4OP^+, 28); IR (cm^{-1}) (CH_2Cl_2, 298 K): 1925 vs; ^{1}H NMR (ppm) ($CDCl_3$, 298 K): 2.40–2.44 (m, 1H), 3.35 (d, 9H, $^3J_{HP}$ = 10.9 Hz), 3.58 (d, 9H, $^3J_{HP}$ = 10.7 Hz), 5.20–5.25 (m, 1H), 6.34–6.36 (m, 1H), 6.74–7.25 (m, 9H); ^{13}C NMR (ppm) ($CDCl_3$, 298 K): 51.3 (d, $^2J_{PC}$ = 5.9 Hz), 51.5 (d, $^2J_{PC}$ = 5.3 Hz), 53.2, 74.2, 95.9, 122.7, 124.3, 126.5, 127.5, 128.0, 130.6, 132.2, 144.6, no CO resonance has been observed; ^{31}P NMR (ppm) ($CDCl_3$, 298 K): 171.8, 180.8.

MS and spectroscopic data of 14. MS (EI): *m/z* (%) 607 (M^+, 17), 539 (? $C_{22}H_{21}F_3NO_6PFe^+$, 7 ?), 455 ($C_{19}H_{21}F_3NO_3PFe^+$, 61), 331 ($C_{16}H_{12}F_3NFe^+$, 100), 304 $((P(OMe)_3)_2Fe^+$, 10), 256 ($C_{16}H_{12}F_2N^+$, 44), 93 $(P(OMe)_2)^+$, 36); IR (cm^{-1}) (CH_2Cl_2, 298 K): 1928 vs; ^{1}H NMR (ppm) ($CDCl_3$, 298 K): 2.39–2.51 (m, 1H), 3.33 (d, 9H, $^3J_{HP}$ = 10.9 Hz), 3.51 (d, 9H, $^3J_{HP}$ = 10.7 Hz), 5.25–5.30 (m, 1H), 6.31–6.33 (m, 1H), 6.86–7.64 (m, 9H); ^{13}C NMR (ppm) ($CDCl_3$, 298 K): 51.4 (br), 53.3, 53.7, 75.5, 94.5, 119.5 (q, $^2J_{CF}$ = 35.0 Hz), 120.7, 124.5, 124.9, 126.6, 127.5 (q, $^1J_{CF}$ = 249.8 Hz), 128.1, 143.0, 158.7, no CO resonance has been observed; ^{31}P NMR (ppm) ($CDCl_3$, 298 K): 171.3, 180.7.

MS and spectroscopic data of 15. MS (EI): *m/z* (%) 675 (M^+, 19), 647 (M^+ – CO, 3), 523 ($C_{20}H_{20}F_6NO_3PFe^+$, 73), 399 ($C_{17}H_{11}F_6NFe^+$, 100), 342 ($C_{17}H_{10}F_6N^+$, 2), 323 ($C_{17}H_{10}F_5N^+$, 13), 304 ($C_{17}H_{10}F_4N^+$, 27), 93 $(P(OMe)_2)^+$, 45); IR (cm^{-1}) (CH_2Cl_2, 298 K): 1929 vs; ^{1}H NMR (ppm) ($CDCl_3$, 298 K): 2.42–2.45 (m, 1H), 3.35 (d, 9H, $^3J_{HP}$ = 10.9 Hz), 3.59 (d, 9H, $^3J_{HP}$ = 10.8 Hz), 5.28–5.33 (m, 1H), 6.29–6.31 (m, 1H), 7.06–7.27 (m, 8H); ^{13}C NMR (ppm) ($CDCl_3$, 298 K): 51.5 (br), 54.3, 76.2, 93.9, 110.4 (br), 120.7 (br), 124.0 (q, $^1J_{CF}$ = 272.5 Hz), 124.6, 126.6, 128.1, 130.8 (q, $^2J_{CF}$ = 32.3 Hz), 142.7, 156.6, 214.8, 215.3, 215.8, 216.2; ^{31}P NMR (ppm) ($CDCl_3$, 298 K): 170.8, 179.8.

Acknowledgement

We gratefully acknowledge financial support by the *Deutsche Forschungsgemeinschaft* (SFB 436).

References

1 W. Imhof, A. Göbel, D. Braga, P. De Leonardis and E. Tedesco, *Organometallics*, 1999, **18**, 736.

2 (*a*) J. Yin, J. Chen, W. Xu, Z. Zhang and Y. Tang, *Organometallics*, 1988, **7**, 21; (*b*) T. N. Danks and S. E. Thomas, *Tetrahedron Lett*, 1988, **29**, 1425; (*c*) T. N. Danks and S. E. Thomas, *J. Chem. Soc., Perkin Trans*, 1990, 761.

3 (*a*) A. J. Pearson, *Acc. Chem. Res*, 1980, **13**, 463; (*b*) R. Grée, *Synthesis*, 1989, 341; (*c*) H.-J. Knölker, *Synlett*, 1992, 371; (*d*) W. R. Roush and C. K. Wada, *J. Am. Chem. Soc.*,1994, **116**, 2151.

4 (*a*) Y. Guari, S. Sabo-Etienne and B. Chaudret, *Eur. J. Inorg. Chem*., 1999, 1047; (*b*) G. Dyker, *Angew. Chem.*, 1999, **111**, 1808; (*c*) D. Berger and W. Imhof, *Chem. Commun*., 1999, 1457; (*d*) D. Berger and W. Imhof, *Tetrahedron*, in the press.

5 (*a*) D. Braga, F. Grepioni, K. F. Biradha, V. R. Pedireddi and G. R. Desiraju, *J. Am. Chem. Soc.*, 1995, **117**, 3156; (*b*) D. Braga and F. Grepioni, *Acc. Chem. Res.*, 1997, **30**, 81; (*c*) D. Braga, F. Grepioni and G. R. Desiraju, *J. Organomet. Chem*., 1997, **548**, 33; (*d*) V. R. Thalladi, H.-C. Weiss, D. Bläser, R. Boese, A. Nangia and G. R. Desiraju, *J. Am. Chem. Soc*., 1998, **120**, 8702.

6 Y. Gu, T. Kar and S. Scheiner, *J. Am. Chem. Soc.*, 1999, **121**, 9411.

7 (*a*) M. O. Albers, N. J. Coville, T. V. Ashworth and E. Singleton, *J. Organomet. Chem*., 1981, **217**, 385; (*b*) F. A. Cotton and R. V. Parsin, *J. Chem. Soc. I*, 1960, 1440; (*c*) W. Strohmeier and F. Müller, *Chem. Ber*., 1969, **102**, 3613; (*d*) W. E. Caroll, F. A. Deeney, J. A. Delaney and F. J. Lalor, *J. Chem. Soc., Dalton Trans.*, 1973, 718.

8 (*a*) G. Sheldrick, SHELXS-86, Universität Göttingen, 1986; (*b*) G. Sheldrick, SHELXL-93, Universität Göttingen, 1993.

9 L. Zsolnai and G. Huttner, XPMA, Universität Heidelberg, 1996.

10 Siemens Analytical Xray Inst. Inc., XP - Interactive Molecular Graphics, v.4.2, 1990.

Footnote

† Part of this work has been presented at the 28th crystallographic course "Crystal Engineering: From Molecules and Crystals to Materials", 12–23 May 1999, Erice, Italy.

Paper b000562m